18. P. Bourges *et al.*, *Phys. Rev. B* **43**, 8690 (1991).
19. See, for example, J. Yu, A. J. Freeman, J. H. Xu, *Phys. Rev. Lett.* **58**, 1035 (1987); J. Yu *et al.*, *Phys. Lett. A* **122**, 203 (1987).
20. W. E. Pickett, *Rev. Mod. Phys.* **61**, 433 (1989); *Phys. Rev. B* **42**, 8764 (1990); _____, H. Krakauer, R. E. Cohen, D. J. Singh, *Science* **255**, 46 (1992).
21. C. A. Balseiro and L. M. Falicov, *Phys. Rev. B* **20**, 4457 (1979).
22. Y. Hasegawa and H. Fukuyama, *Jpn. J. Appl. Phys.* **26**, L322 (1987).
23. T. Ishiguro and K. Yamaji, *Organic Superconductors* (Springer-Verlag, Berlin, 1990).
24. N. Bulut, D. Hone, D. J. Scalapino, N. E. Bickers, *Phys. Rev. Lett.* **64**, 2723 (1990); *Phys. Rev. B* **41**, 1797 (1990).
25. J. P. Lu, Q. M. Si, J. H. Kim, K. Levin, *Phys. Rev. Lett.* **65**, 2466 (1990).
26. N. Bulut, in *Dynamics of Magnetic Fluctuations in High-Temperature Superconductors*, G. Reiter, Ed. (Plenum, New York, 1990), p. 97, and references cited therein.
27. J. P. Lu, Q. M. Si, J. H. Kim, K. Levin, *Physica C* **179**, 191 (1991).
28. S. V. Maleyev, *J. Phys. I* (*France*) **2**, 181 (1992).
29. N. Bulut and D. J. Scalapino, *Phys. Rev. Lett.* **68**, 706 (1992); *Phys. Rev. B* **45**, 2371 (1992).
30. T. Tanamoto, K. Kuboki, H. Fukuyama, *J. Phys. Soc. Jpn.* **60**, 3072 (1991).
31. P. A. Lee and N. Read, *Phys. Rev. Lett.* **58**, 2691 (1987).
32. J. Ruvalds and A. Virosztek, *Phys. Rev. B* **43**, 5498 (1991).
33. S. Wermbter and L. Tewordt, *ibid.*, p. 10530.
34. J. W. Serene and D. W. Hess, *ibid.* **44**, 3391 (1991).
35. J. M. Tranquada *et al.*, in preparation; B. J. Sternlieb *et al.*, in preparation.
36. C. M. Varma *et al.*, *Phys. Rev. Lett.* **63**, 1996 (1989); G. Kotliar *et al.*, *Europhys. Lett.* **15**, 655 (1991).
37. B. S. Shastry and B. I. Shraiman, *Phys. Rev. Lett.* **65**, 1068 (1990).
38. A. Virosztek and J. Ruvalds, *ibid.* **67**, 1657 (1991).
39. B. H. Grier, G. Shirane, S. A. Werner, *Phys. Rev. B* **31**, 2892 (1985); E. Fawcett, S. A. Werner, A. Goldman, G. Shirane, *Phys. Rev. Lett.* **61**, 558 (1988).

40. We appreciate helpful information from H. Monien, G. Aeppli, M. Kastner, and J. M. Tranquada. This research was supported by Department of Energy grant DE-FG05-84ER45113 and by Hungarian National Research Fund grants OTKA 2950 and T4473.

26 February 1992; accepted 27 April 1992

Soluble Aluminum Silicates: Stoichiometry, Stability, and Implications for Environmental Geochemistry

B. A. Browne and C. T. Driscoll

Soluble aluminum silicate (Al-Si) complexes are critical species for the development and application of geochemical models. A fluorescence probe technique was used to show that Al-Si complexes account for up to 95% of the total inorganic mononuclear Al in natural waters. The presence of these soluble Al-Si species affects the solubility of Al-Si minerals. Soluble Al-Si species may be important intermediates in the weathering reactions of primary Al-Si minerals and should be considered in dissolution models. Soluble Al-Si species may be key components controlling the formation of metastable and new stable minerals during interactions between water and rocks or soils.

Despite an abundance of Al and H-silicate (H_4SiO_4) ions in natural solutions in contact with Al-Si surfaces in soil and geological formations (*1*), little attention has been accorded to soluble Al-Si species. Soluble Al-Si species may be intermediate in the decomposition of activated complexes (*2*) formed on the surfaces of minerals (for example, potassium-feldspar) during the hydrolytic reaction in aqueous solutions and may play a key role in the formation of metastable and new stable minerals during rock-water and soil-water interactions. Consideration of soluble Al-Si is critical for the development and application of geochemical and soil models. In this report, we characterize the significance and thermodynamic stability of a 1:1:0 Al:Si:OH complex and of 2:2:*r* and 2:1:*r* Al-Si species.

We applied a fluorescence probe technique (*3*) to characterize low-order (mononuclear and dinuclear) soluble Al-Si species. Aluminum and Si were combined at low concentrations in dilute acidic solutions of the fluorescence reagent morin (Table 1) (*4*). We measured concentrations of Al^{3+} and total silicate–bound Al (Al-Si) by comparing the fluorescence signal to that of solutions lacking Si (*4*). Because the Al-morin complexes give a large fluorescence signal, the fraction of total soluble Al responsible for the fluorescence signal can be maintained at a low value (typically less than 10%) in the analysis. The method is thus sensitive to subtle differences in the equilibrium distribution of soluble Al, an outcome that has not been achieved with other methods for the analysis of Al. Stability constants for aqueous aluminum fluoride and aluminum sulfate complexes measured by the morin technique compare favorably to published values (*4*).

We evaluated the stoichiometry of Al-Si according to the following reaction series, allowing for the formation of mixed hydroxy-Al-silicates:

$$pAl^{3+} + qH_4SiO_4 + rH_2O = Al_p(OH)_r(OSi(OH)_3)_q^{3p-q-r} + (q + r)H^+ \tag{1}$$

where p, q, and r are stoichiometric coefficients. From Eq. 1, the equilibrium concentration of the pqrth complex is given by:

$$[Al_p(OH)_r(OSi(OH)_3)_q^{3p-q-r}] = K_{pqr}(\tau_3/\tau_{3p-q-r})[Al^{3+}]^p[H_4SiO_4]^q\{H^+\}^{-(q+r)} \tag{2}$$

where K_{pqr} is the equilibrium constant for the pqrth complex, brackets signify concentration, braces signify activity, and τ_i symbolizes the activity coefficient for an Al species. The total concentration of Al-Si at equilibrium may be described in terms of measured reaction variables ($[Al^{3+}]$, $[H_4SiO_4]$, and $\{H^+\}$):

$$[\text{Al-Si}] = \sum_{1}^{P}\sum_{1}^{Q}\sum_{0}^{R} pK_{pqr}(\tau_3/\tau_{3p-q-r}) [Al^{3+}]^p[H_4SiO_4]^q\{H^+\}^{-(q+r)} \tag{3}$$

Table 1. Summary of maximum stoichiometric coefficients (Eq. 4) for Al (P), Si (Q), and H_2O (R) observed in the experiments (25° ± 0.1°C, 0.01 M ionic strength, 0.001 M CH_3COO^-, 1 μM total morin) and proposed stoichiometries of Al-Si species. *n* is the number of samples.

n	pH	H_4SiO_4 (mM)	Total Al (μM)	Maximum stoichiometric coefficient			Proposed species stoichiometries (*p*,*q*,*r**)
				P	*Q*	*R*	
16	4.0	0.10	0.64–10.3	1	1	0	1,1,0
16	4.0	0.26	0.64–10.3	1	1	0	1,1,0
16	4.5	0.10	0.64–10.3	1	1	0	1,1,0
16	4.5	0.27	0.64–10.3	1	1	0	1,1,0
32	5.0	0.11	0.64–10.3	1	1	0	1,1,0
13	5.5	0.11	0.26–4.07	2	2	2*	1,1,0; 2,1,2*; 2,2,2*
13	5.5	0.25	0.26–4.07	2	2	2*	1,1,0; 2,1,2*; 2,2,2*

*Based on 2:1:2 and 2:2:2 Al·Si:OH mineral analogs imogolite and allophane.

B. A. Browne, School of the Environment, Duke University, Durham, NC 27706.

C. T. Driscoll, Department of Civil and Environmental Engineering, Syracuse University, Syracuse, NY 13244.

where P, Q, and R are maximum stoichiometric coefficients (Table 1). If both sides of Eq. 3 are divided by $[Al^{3+}]$ and $[H_4SiO_4]$, a similar polynomial expression describing the extent of complex formation may be derived:

$$K_{Al\text{-}Si} = \sum_{1}^{P} \sum_{1}^{Q} \sum_{0}^{R} pK_{pqr}(\tau_3/\tau_{3p-q-r}) \\ [Al^{3+}]^{p-1}[H_4SiO_4]^{q-1}\{H^+\}^{-(q+r)} \quad (4)$$

Using Eq. 4, we established the value of P at each pH and $[H_4SiO_4]$ combination (Table 1) from a plot of $K_{Al\text{-}Si}$ as a function of $[Al^{3+}]$. The mean $K_{Al\text{-}Si}$ values shown in Fig. 1A reflect only mononuclear terms ($P = 1$ in Eq. 4: $\Sigma\Sigma K_{1qr}\tau_{3-q-r}[H_4SiO_4]^{q-1}\{H^+\}^{-(q+r)}$) at pH 4.0, 4.5, and 5.0, and predominantly mononuclear terms at pH 5.5. The mean values of $K_{Al\text{-}Si}$ at pH 4.0 and 4.5 were essentially unaffected by $[H_4SiO_4]$. These data indicate (by Eq. 4) that the stoichiometric coefficient $Q = 1$ for the mononuclear species is a maximum.

The mean values for $K_{Al\text{-}Si}$ were highest at pH 5.5 (Fig. 1A). The upward curvilinear trend with pH reflects H^+ displacement from H_4SiO_4 by Al^{3+}. When $K_{Al\text{-}Si}$ values were adjusted to account for this deprotonation, they were essentially identical at each pH (Fig. 1B). This result suggests that additional H^+-producing reactions were absent in the formation of the mononuclear Al-Si. Hence, mononuclear hydroxy-Al-silicates were not detectable in the experimental solutions.

From these results, we infer the following mononuclear reaction:

$$Al^{3+} + H_4SiO_4 = \\ Al(OSi(OH)_3)^{2+} + H^+ \quad (5)$$

where the stoichiometric equilibrium constant is given by:

$$K_{110} = \frac{[Al(OSi(OH)_3)^{2+}]\tau_2\{H^+\}}{[Al^{3+}]\tau_3[H_4SiO_4]} \quad (6)$$

We evaluated the $Al(OSi(OH)_3)^{2+}$ model by linear least-squares fit of the data (Fig. 1C) to the following logarithmic transformation of Eq. 6:

$$-\log(Y) = -\log(K_{110}) - \log([Al^{3+}]) \quad (7)$$

where $Y = ([Al(OSi(OH)_3)^{2+}]\tau_2\{H^+\}/\tau_3[H_4SiO_4])$. The slope ($0.98 \pm 0.03$, $P < 0.0001$) from the analysis was close to the theoretical slope of 1; this result confirms adherence to the model and indicates that mononuclear species predominate over polynuclear species under the experimental conditions. This pattern also confirms that mononuclear hydroxy-Al-silicates ($p = 1$, $r > 0$) and higher order silicates ($p = 1$, $q > 1$) are absent under the experimental conditions.

Our estimates of pK_{110} and the free energy of formation ($G^{0}_{f,298}$) of $Al(OSi(OH)_3)^{2+}$ were 1.07 ± 0.06 and -428.21 ± 0.08 kcal/mol, respectively (5). Theoretical $Al(OSi(OH)_3)^{2+}$ formation curves for Si concentrations common in natural waters suggest that $Al(OSi(OH)_3)^{2+}$ will be a prominent inorganic species of mononuclear Al under acidic conditions (Fig. 2A). A total of 216 samples (6) were analyzed from first-order streams of the Hubbard Brook Experimental Forest (HBEF) in the White Mountains of New Hampshire ($n = 104$), the Jamieson Creek Watershed (JCW) in the Cascade Mountains of British Columbia ($n = 43$), and the North Branch of the Moose River (NBMR) in the Adirondack Mountains of New York ($n = 69$). Speciation measurements for these dilute acidic natural waters (Fig. 2B) show that formation of $Al(OSi(OH)_3)^{2+}$ will affect the species distribution of soluble Al even at low Si concentrations.

We inferred that there were two dinuclear Al-Si stoichiometries from the experimental data at pH 5.5 (7): a 2:1 Al:Si combining ratio (8) and a 2:2 Al:Si combining ratio. If by analogy to imogolite and kaolinite the bridging ligand between Al atoms is assumed to be OH^-, the stoichiometric coefficient of OH would result in 2:1:2 and 2:2:2 Al:Si:OH species, respectively. Formation of these species is given by:

$$2Al^{3+} + qH_4SiO_4 + 2H_2O = \\ Al_2(OH)_2(OSi(OH)_3)^{(4-q)} + (2 + q)H^+ \quad (8)$$

The stability constants, $K_{(2,2,2)}$ and $K_{(2,1,2)}$, for the individual species were estimated to be 1.9×10^{-7} and 7.7×10^{-6}, respectively, at pH 5.5 (9). Inclusion of OH as the bridging ligand in this reaction model conveys the importance of low-order polynuclear hydroxy Al (OH-Al) ions in the formation of soluble Al-Si. The importance of these ions can be seen if we recast Eq. 8 in terms of the dinuclear OH-Al ions:

$$Al^2(OH)_2{}^{4+} + qH_4SiO_4 = \\ Al_2(OH)_2(OSi(OH)_3)^{(4-q)} + (q)H^+ \quad (9)$$

Factors that lead to the achievement of the activation energy necessary to attain equilibrium with polynuclear OH-Al ions re-

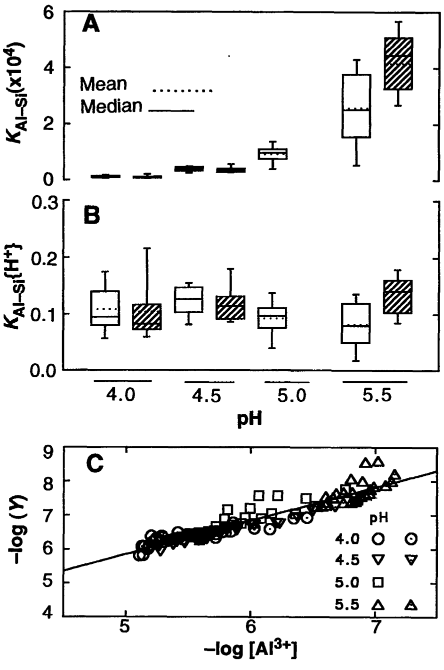

Fig. 1. Relation between reaction variables and experimental conditions (Table 1). Error bars represent 10th and 95th percentiles. Boxes represent the interquartile range. (**A**) Summary of $K_{Al\text{-}Si}$ values (Eq. 4) for each pH and Si combination. Open and hatched boxes reflect low and high Si concentrations, respectively. (**B**) Values of $K_{Al\text{-}Si}$ adjusted for one H^+ displaced from H_4SiO_4 by Al^{3+}. (**C**) Fit of the data to the $Al(OSi(OH)_3)^{2+}$ reaction model given in Eq. 7. Symbols with and without dots represent high and low $[H_4SiO_4]$, respectively.

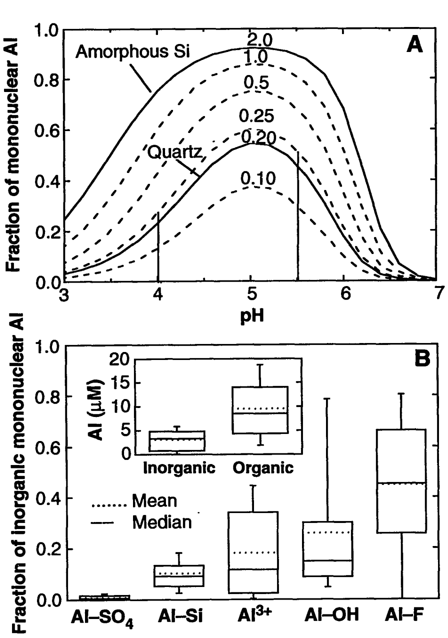

Fig. 2. (**A**) Theoretical formation curves for $Al(OSi(OH)_3)^{2+}$ (fraction of total mononuclear Al) in dilute (ionic strength = 0.001 M) acidic aqueous solutions of H_4SiO_4. The value of $[H_4SiO_4]$ for each line is given in millimoles per liter. The area delimited by the vertical lines represents the pH and $[H_4SiO_4]$ range of our experiments. Approximate lower and upper limits of complex formation expected in natural waters are shown on the basis of the solubility limits of quartz and amorphous silica, respectively. The presence of other Al-binding ligands in natural waters (for example, F^- and fulvic acids) will reduce the formation of $Al(OSi(OH)_3)^{2+}$ at a given concentration of H_4SiO_4. (**B**) Species distribution ($n = 216$) of inorganic mononuclear Al in dilute acidic natural waters (*6*). Box plots represent the interquartile range, error bars represent the 10th and 95th percentiles. Inset illustrates the distribution between inorganic and organic mononuclear Al.

main poorly understood (*10*). Such factors will likely exert similar constraints on spontaneous formation of polynuclear hydroxy-Al-silicates. Hence, they may confound development of accurate thermodynamic data for polynuclear hydroxy-Al-silicates until they are elucidated.

The equilibrium chemistry of soluble Al-Si species may affect accurate characterization and modeling of the thermodynamic stability fields of Al-Si minerals. To explore this hypothesis, we recalculated solubility data reported by May *et al.* (*11*) for kaolinite and smectite suspensions to include formation of $Al(OSi(OH)_3)^{2+}$. It was assumed that the $Al(OSi(OH)_3)^{2+}$ species was measured as part of total mononuclear Al. Soluble Al-Si accounted for approximately 10 to 30% of the total mononuclear Al in the kaolinite suspensions (Fig. 3B) and approximately 47 to 86% in the smectite suspensions (Fig. 3G). Inclusion of the soluble Al-Si species in the solubility calculations improved the fit of the kaolinite suspension data to the theoretical equilibrium solubility of kaolinite (Fig. 3, A and D) and resulted in a lower value of the solubility product constant and a smaller variance (Fig. 3C). Adjustment of the experimental data to include soluble Al-Si species also significantly affected interpretation of the observations of May *et al.* (*11*) of smectite suspensions at pH 5 (*12*). The apparent mineral phase controlling the solubility shifted from amorphous or crystalline aluminum hydroxides (*11*) (Fig. 3, E and H) to kaolinite (Fig. 3, F and H). These results suggest that the true solubility of Al-Si minerals may be masked without consideration of soluble Al-Si species. Until sufficient knowledge of soluble Al-Si species is developed, it remains to be determined (i) whether reliable equilibrium solubilities and solubility-derived G_f^0 values for solid aluminum silicates can be obtained by conventional experimental procedures for mineral-water interactions and (ii) to what degree existing solubility data reflect undetected formation of soluble Al-Si species (*13*).

The systematics of dissolution-precipitation reactions involving aluminum silicates during rock-water and soil-water interactions are being established. We can now begin to evaluate the qualitative and quantitative significance of soluble Al-Si species in these interactions. We propose that soluble Al-Si species are intermediates in the weathering reactions of primary and secondary aluminum silicates in soils, geological formations, and surface waters. They may affect the dissolution of solid aluminum silicate and serve as templates, or structural subunits, for secondary clay minerals. Further evaluation of stoichiometric concepts implicit in congruent and incongruent dissolution models of Al-Si minerals (*14*) is needed and the significance of soluble Al-Si species in silicate·dissolution mechanisms (*15*) must be considered.

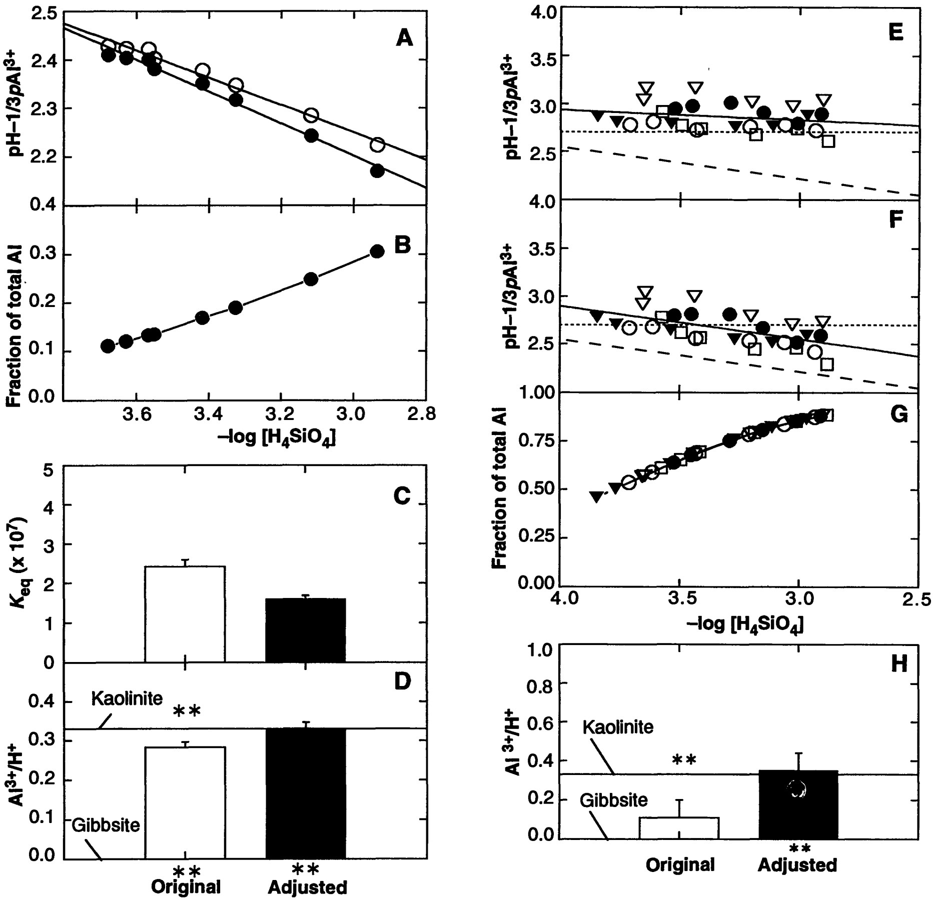

Fig. 3. Kaolinite (pH 4, A to D) and smectite (pH 5, G to H) aqueous solubility experiments reported by May *et al.* (*11*) adjusted for $Al(OSi(OH)_3)^{2+}$ formation. (**A**) Original (open circles) and adjusted (closed circles) solution composition data for Dry Branch kaolinite. There is a significant difference ($P < 0.01$) in the apparent dissolution stoichiometry of kaolinite between the original and adjusted data [see (D)]. (**B** and **G**) Fraction of total soluble Al as $Al(OSi(OH)_3)^{2+}$. (**C**) Solubility product constants for the original and adjusted data (error bars represent 1 SE) were significantly different ($P < 0.01$). (**D** and **H**) Measured stoichiometric dissolution ratios (moles of Al released per H^+ consumed) and ideal values for kaolinite and gibbsite. Error bar represents 1 SE. Symbol (**) indicates a statistically significant difference ($P < 0.01$) between the measured and ideal stoichiometric ratios. (**E** and **F**) Original and adjusted solution composition data, respectively, for five (pH 5) smectite suspensions [Panther Creek (open circles), Lualualei (closed circles), St. Louis Heights (triangles), Kokokahi (closed triangles), Upton (open squares)] (———, regression line). Phase boundaries for gibbsite (. . . . . .) and kaolinite (- - - -) reference minerals are shown.

REFERENCES AND NOTES

1. J. D. Hem, *U.S. Geol. Surv. Water Supply Pap. 1473* (1970); D. E. White, J. D. Hem, G. A. Waring, *U.S. Geol. Surv. Water Supply Pap. 440-F* (1963); H. J. M. Bowen, *Environmental Chemistry of the Elements* (Academic Press, London, 1979).
2. P. Aagaard and H. C. Helgeson, *Am. J. Sci.* **282**, 237 (1982).
3. B. A. Browne, J. G. McColl, C. T. Driscoll, *J. Environ. Qual.* **19**, 65 (1990); B. A. Browne, C. T. Driscoll, J. G. McColl, *ibid.*, p. 73.
4. The H^+ activity was calculated from pH values measured to a precision of ±0.01. The activity of free silicic acid was estimated from the known total concentration of silicate ((H_4SiO_4) = [total Si] – [Al-Si]). We estimated the activity coefficients for silicate-bound Al and Al^{3+} using the Davies and extended Debye-Huckel equations [W. Stumm and J. J. Morgan, *Aquatic Chemistry* (Wiley, New York, 1981), p. 135], respectively.
5. The minimum variance formula of S. L. Meyer [*Data Analysis for Scientists and Engineers* (Wiley, New York, 1975)] was used to calculate the best estimates of the stability constant of $Al(OSi(OH)_3)^{2+}$. Because the presence of the dinuclear Al-Si species could confound the result, the experimental data for pH 5.5 were excluded from the calculations. However, inclusion of the pH 5.5 data in the calculations had little effect on the mean value.
6. The overall mean ± standard deviation values for pH and concentrations were as follows: pH = 5.0 ± 0.6, total mononuclear Al = 13 ± 8 μM, H_4SiO_4 = 82 ± 21 μM, dissolved organic carbon = 470 ± 319 μM, fluoride = 3 ± 2 μM, and sulfate = 57 ± 20 μM. Site descriptions are given in the following: HBEF, C. T. Driscoll, N. van Breemen, J. Mulder, *Soil Sci. Soc. Am. J.* **49**, 437 (1985); JCW, N. M. Johnson, in *Geological Aspects of Acid Deposition*, O. P. Bricker, Ed. (Butterworth, Boston, 1984), pp. 37–53; NBMR, C. T. Driscoll, C. P. Yatsko, F. J. Unangst, *Biogeocheimstry* **3**, 37 (1987). Details of the samples' water chemistry are in B. A. Browne, thesis, Syracuse University (1988).

7. Linear plots of $K_{Al\text{-}Si}$ as a function of $[Al^{3+}]$, consistent with the presence of dinuclear Al ($P = 2$, Eq. 4) as a small fraction of total Al, were obtained for low (0.11 mM) and high (0.25 mM) $[H_4SiO_4]$ at pH 5.5. From Eq. 4 the slope of these plots is given by

$$m = \Sigma\Sigma K_{2qr}(\tau_3/\tau_{6-q-r})[H_4SiO_4]^{q-1}\{H^+\}^{-(q+r)}$$

Hence, for the case of exclusively one stoichiometry of silica for the dinuclear species, the slope ratio $m' = m_{0\,25}/m_{0\,11}$ is given by the ratio of the two concentrations raised to the $q - 1$ power $(0.25/0.11)^{(q-1)}$ or 2.27 ($q-1$). Values of m' for $q = 1$, $q = 2$, and $q = 3$ are 1, 2.27, and 5.15, respectively. The actual ratio was 1.72 for slope values of $1.8 \times 10^{11} \pm 3.7 \times 10^{10}$ (0.11 mM Si) and $3.1 \times 10^{11} \pm 8.5 \times 10^{10}$ (0.25 mM Si). Theoretically, at least two dinuclear species, including necessarily a 2:1 Al:Si species, would therefore have been present. The silica stoichiometry of the second species was assumed to be 2 by analogy to kaolinite.

8. The 2:1 Al:Si stoichiometry is noteworthy because it is consistent with the stoichiometry of protoimogolite (a positively charged hydroxy-Al-silicate sol) described by Farmer and co-workers as a proposed explanation for the development of the B_s horizon of podzolic soil profiles [V. C. Farmer, J. D. Russel, M. L. Berrow, *J. Soil Sci.* **31**, 673 (1980); V. C. Farmer, *Coloq. Int. CNRS* **303**, 275 (1981); *Soil Sci. Plant Nutr.* (*Tokyo*) **28**, 571 (1982); in *Podzols et Podzolization*, D. Righi and A. Chauvel, Eds. (Assoc. Fr. Estude Sol, Plaisir, France, 1987, pp. 187–194)].

9. The estimates of $K_{(222)}$ and $K_{(212)}$ were generated by simultaneous solution of two equations of the form

$$m_{\{H_4SiO_4\}} = (\tau_3/\tau_3)K_{212}\{H^+\}^{-3} + \tau_3\tau_2 K_{222}\{H^+\}^{-4}[H_4SiO_4]$$

where from Eq. 4 the general form of $m_{[H_4SiO_4]}$, given by $\tau_3/\tau_{6-q-r}\Sigma\Sigma K_{2qr}[H_4SiO_4]^{q-1}\{H^+\}^{-(q+r)}$, represents the slope of plots of $K_{Al\text{-}Si}$ as a function of $[Al^{3+}]$ for the case of $P = 2$. The experimentally determined values of $m_{[H_4SiO_4]}$ for 0.11 and 0.25 mM $[H_4SiO_4]$ were $1.8 \times 10^{11} \pm 3.7 \times 10^{10}$ and $3.1 \times 10^{11} \pm 8.5 \times 10^{10}$, respectively.

10. We have a poor understanding of the kinetic and thermodynamic characteristic of polynuclear OH-Al ions, and little is known of low-order species such as dinuclear OH-Al ions. Compositions and structures remain controversial [P. H. Hsu, in *Minerals in Soil Environments* (Soil Science Society of America, Madison, WI, 1989), pp. 331–378; P. M. Bertsch, *Soil Sci. Soc. Am. J.* **51**, 825 (1987)], and widely varying rates of hydrolysis and nucleation of Al^{3+} have been reported in response to different solution conditions. Most laboratory studies have been conducted at high Al^{3+} concentrations, which tend to obscure the reactions of low-order polynuclear OH-Al ions, and Bertsch has shown that the observed distributions of Al between mononuclear and polynuclear forms are artifacts of synthesis conditions.

11. H. M. May, D. G. Kinniburgh, P. A. Helmke, M. L. Jackson, *Geochim. Cosmochim. Acta* **50**, 1677 (1986). The kaolinite samples studies by May *et al.* were from Dry Branch, GA. Of the smectite samples they studied, two (Upton, WY, and Panther Creek, MO) were from commercial bentonite deposits and the remaining three (Kokokahi, Lualualei, and St. Louis Heights) were samples of the A horizons from Hawaiian Vertisols.

12. We conducted similar calculations for the data of May *et al.* (*11*) on smectite suspensions at pH 6 and 7 but obtained little effect. This result is not surprising because $Al(OSi(OH)_3)^{2+}$ and the dinuclear hydroxy-Al-silicates are unable to compete with OH-Al ions at these pH values. Other soluble hydroxy-Al-silicates may exist that could improve the conformance of the data of May *et al.* (*11*) to smectite phase boundaries at these pH values. However, additional studies are needed to characterize their stoichiometry and stability.

13. Similar implications may apply for the interpretation of weathering experiments. One could propose that the nonstoichiometric release of Al and Si observed in several recent experiments on the dissolution of silicates [L. Chou and R. Wollast, *Geochim. Cosmochim. Acta* **48**, 2205 (1984); G. R. Holdren and R. A. Berner, *Am. J. Sci.* **285**, 994 (1985)] may reflect the stoichiometry of undetected soluble polynuclear Al-Si species. For example, a 2:1 (Al:Si) soluble Al-Si species formed in or released to solution could result in an apparent stoichiometric excess of Al over silica in the solution phase and a layer enriched in silica on the surface of the mineral.

14. It is implicit in congruent and incongruent dissolution models of aluminosilicate minerals that dissolution reactions proceed directly to Al^{3+} without soluble Al-Si intermediates. Such intermediate species could have important roles in mineral transformation or neoformation reactions.

15. Relations between solid Al-Si species and their soluble Al-Si alteration products may be fundamental features of weathering mechanisms. Summary discussions of current perspectives on weathering mechanisms are given by P. R. Bloom and A. E. Nater [in *Rates of Soil Chemical Processes, SSSA Special Publication 27*, D. L. Sparks and D. L. Suarez, Eds. (Soil Science Society of America, Madison, WI, 1991), chap. 7]; S. M. Colman and D. D. Dethier [in *Rates of Chemical Weathering of Rocks and Minerals*, S. M. Colman and D. D. Dethier, Eds. (Academic Press, New York, 1986), pp. 1–20]; and J. Schott and J. C. Petit [in *Aquatic Surface Chemistry*, W. Stumm, Ed. (Wiley, New York, 1987), pp. 293–315].

16. This work was supported by a Presidental Young Investigator Award to C.T.D. Funds were provided by the National Science Foundation, the Empire State Electric Energy Research Corporation, and the Electric Power Research Institute. This is a contribution of the Hubbard Brook Ecosystem Study.

7 February 1992; accepted 27 April 1992

Morphological Disparity in the Cambrian

Derek E. G. Briggs, Richard A. Fortey, Matthew A. Wills

An analysis of the range of morphology among arthropods demonstrates that disparity among living arthropods is similar to that in Cambrian arthropods. The range of morphological design resulting from the Cambrian "explosion" has been overestimated, reflecting a tendency to separate as "problematic" taxa that cannot be accommodated in the classification on the basis of the living biota. Problematic taxa are largely an artifact of an inadequate taxonomy. Special evolutionary processes may not be necessary to explain the early radiation of the metazoans.

Early metazoan fossils that preserve nonmineralized tissues, such as those of the Middle Cambrian Burgess Shale (*1*), include a range of animals that do not fit readily into higher taxa that are based on the living fauna. This has led to claims about the special place of Cambrian organisms in metazoan history, including the assertion that among the Cambrian faunas are many representatives of higher taxa—even "phyla"—that no longer survive (*2*) and that the variety of different body plans was much more extensive in the Cambrian than it is now (*3*). This range of design is termed "disparity" to distinguish it from "diversity," which is measured as number of species or genera (*3*, *4*). There is ample evidence that the Cambrian animals appeared within a relatively short interval of geological time. Thus, the question of whether they show greater disparity than living faunas has important implications for our interpretation of rates of morphological change during the Cambrian. It has been argued, for example, that special genetic mechanisms would have been necessary to achieve what appear to be high degrees of disparity (*3*, *5*).

The arthropods are the most important group in the Burgess Shale in terms of numbers of genera and of individuals (*6*). They are complex enough and preserve sufficient characters to provide credible comparisons with living representatives. Few arthropods from Burgess Shale–type faunas can be assigned readily to one of the four major groups: the Crustacea, Chelicerata, Uniramia, and the extinct Trilobita (*7*). Over 20 genera lack the diagnostic characters of these groups and have therefore been termed problematica. The suggestion that these problematica represent at least 20 unique designs equivalent in rank to the crustaceans, chelicerates, uniramians, and trilobites (*3*) has been a linchpin in models of enormous Cambrian disparity.

Disparity is a difficult concept to define in quantitative terms. Multivariate morphometric assessments of shape or change in shape (*8*) provide the most objective measure. Such an approach has demonstrated that both morphologic dispersion and distinctness of suprageneric taxa (superfamilies) of trilobites increased from the Cambrian to the late Ordovician (*9*). Likewise, morphologic diversity of the blastoid echinoderms essentially increased to the Permian, when they became extinct, in

---

D. E. G. Briggs and M. A. Wills, Department of Geology, University of Bristol, Wills Memorial Building, Queen's Road, Bristol BS8 1TR, United Kingdom.
R. A. Fortey, Department of Palaeontology, Natural History Museum, Cromwell Road, London SW7 5BD, United Kingdom.